BDX-613-1716 (Rev.)

DETERMINATION OF GOLD-COPPER ALLOY COMPOSITION BY X-RAY FLUORESCENCE ANALYSIS

PDO 6984809, Final Report

D. M. Starks, Project Leader

Published September 1977

Prepared for the United States Energy Research and Development Administration Under Contract Number EY-76-C-04-0613 USERDA

Bendix Kansas City Division

DISCLAIMER

NOTICE

Printed in the United States of America

Available From the National Technical Information Service, U.S. Department of Commerce, 5285 Port Royal Road, Springfield, Virginia 22161.

Price: Microfiche $2.25
Paper Copy $4.~~00~~ 50

BDX-613-1716 (Rev.)
Distribution Category UC-38

DETERMINATION OF GOLD-COPPER ALLOY COMPOSITION BY X-RAY FLUORESCENCE ANALYSIS

Published September 1977

Project Leader:
D. M. Starks
Department 812

PDO 6984809
Final Report

Communications Services

Bendix Kansas City Division

DETERMINATION OF GOLD-COPPER ALLOY COMPOSITION BY X-RAY FLUORESCENCE ANALYSIS

BDX-613-1716 (Rev.), UNCLASSIFIED Final Report, Published September 1977

Prepared by D. M. Starks, D/812, Under PDO 6984809

The development of a technique for in-process determination of the composition of electroplated gold-copper by X-ray fluorescence analysis is described. The principle of X-ray fluorescence spectroscopy and the operation of a source-excited, non-dispersive X-ray fluorescence analyzer are discussed. A calibration technique which makes use of standards with known alloy composition is presented, and the use of this technique, along with the precision and accuracy achieved, for in-process analysis is discussed.

WPC-dkvh

The Bendix Corporation
Kansas City Division
P.O. Box 1159
Kansas City, Missouri 64141

A prime contractor with the United States Energy Research and Development Administration under Contract Number EY-76-C-04-0613 USERDA

CONTENTS

ILLUSTRATIONS

TABLE

SUMMARY

A method for in-process determination of the composition of electroplated gold-copper alloys using X-ray fluorescence analysis has been developed. The technique makes use of the fact that when a material is suitably irradiated, the atoms of the constituent elements give off fluorescent radiation of characteristic energies. Since the intensity of the radiation from an element contained in a sample is directly proportional to the amount of that element present, the development of calibration techniques permits a quantitative analysis of the sample.

A source-excited, non-dispersive X-ray fluorescence analyzer was procured and developed for this purpose. A set of calibration standards was procured, and a calibration curve was constructed by plotting a ratio of X-ray fluorescence intensities against known alloy composition.

This technique is now being used as the primary method for in-process alloy measurements during gold-copper electroplating. It replaces a previously used technique involving the calculation of the mass density of the plated deposit. The X-ray technique has been shown to measure alloy composition to an overall precision of ±0.12 weight percent using two-minute counting times. Post-plate D-tests of parts from full length plating runs show the X-ray technique to agree with electron microprobe analysis within the limits of precision.

DISCUSSION

SCOPE AND PURPOSE

An improved technique was needed for in-process determination of the alloy composition of electroplated gold-copper. The technique was required to be fast, nondestructive, and at least as precise as the formerly used method. Quantitative analysis by X-ray fluorescence spectroscopy appeared to meet these requirements. The scope of this work included the purchase of a radioactive isotope source-excited, non-dispersive X-ray fluorescence analyzer and the development of calibration and data analysis procedures permitting its use for in-process determination of gold-copper alloy composition. The bulk of the activity reported herein occurred during FY75 and was funded by PDO 6984809.

ACTIVITY

Background

In-Process Determination of Alloy Composition of Gold-Copper Electrodeposits

Electroplating of gold-copper alloys as performed at Bendix requires periodic in-process determination of alloy composition and adjustment of control parameters. This has been performed in the past by determination of the mass density of the plated deposit and correlation of this density with alloy composition. This procedure has significant limitations. Because of large relative errors in the size measurement, meaningful density values cannot be calculated for less than approximately 0.2 mm of deposit thickness, which corresponds to about 24 hours of plating. Thus, the length of time required for an alloy control test run may be several days, since a 24-hour period is required to evaluate a single process control setting. In addition, any controlled variation of alloy composition over a time interval of less than 24 hours is impossible since the density represents the average composition plated during this period and cannot identify short term variations. Other disadvantages include the fact that the density measurement is sensitive to operator error and temperature variations.

X-ray fluorescence analysis appears to overcome the essential limitations of the density technique. It is a non-destructive method which analyzes a relatively thin layer of material at the surface of a sample. Therefore, meaningful in-process measurements may be made at frequent intervals. This shortens the length of time required for alloy control test runs, and permits

the plating of alloys with controlled short-term variations. The technique is insensitive to plating geometry and temperature variations and is relatively immune from operator error. Once the equipment is set up and calibration techniques are developed, an analysis can be carried out quickly and easily.

X-Ray Fluorescence Spectroscopy

When an element is exposed to radiation of suitable energy, transitions occur in the electron energy levels in the atoms of the element which cause it to emit fluorescent radiation having a characteristic energy spectrum. Radiation in the X-ray region of the electromagnetic energy spectrum excites fluorescent radiation in the same region. Since each element has a unique X-ray energy spectrum, the identity of the various elements present in an unknown sample can be determined by observing the specific energies present in the emitted fluorescent radiation. In addition, since the intensity of the fluorescence from an element is directly proportional to the amount of that element present in a sample, measurement of this intensity provides a means for determining the amount of the element present. The measurement of the energy and intensity of fluorescent X-rays is termed X-ray fluorescence analysis and is an important nondestructive technique for qualitative and quantitative analysis of solids and liquids.

The specific X-ray energies making up the characteristic spectrum of an element are identified by letters and subscripts which denote the energy level transitions that create them. For example, when the exciting radiation ejects a K-shell electron from the atom, the vacancy in the K-shell can be filled by an electron from a higher shell. When this occurs, an X-ray photon is produced. Since the vacancy was created in the K-shell and an electron moved to the K-shell to fill it, the resulting X-ray is identified as a K X-ray. If the electron that made the transition came from the next higher shell (the L-shell), it is denoted by an α, and the resulting X-ray is a Kα. If the electron was from the second higher energy level (the M-shell), the designation would be Kβ. The same notation applies to transitions between higher levels. For example, a transition to the L-shell from the M-shell would be designated Lα. Designations with numerical subscripts such as Kβ_1 denote specific transitions involving subshells within the primary energy levels.

Detailed X-ray spectra of the elements are typically tabulated in units of electron volts (eV) or thousands of electron volts (keV). The elements contained in an unknown sample may be identified by comparison of the X-ray spectrum determined by the fluorescence analyzer with tabulated X-ray spectra of the elements. X-ray intensity measurements may then be made for the particular elements of interest.

Equipment

X-ray fluorescence analysis requires a source of radiation to excite the fluorescence and a means of measuring the fluorescent energy and intensity. The first X-ray fluorescence analysis systems used a high-voltage X-ray tube to provide the excitation and an X-ray crystal spectrometer to measure the fluorescence. This measurement is accomplished by diffracting the fluorescent X-rays from a crystal of known lattice spacing. The angle through which an X-ray is diffracted depends upon its wavelength (and therefore its energy), and fluorescent radiation consisting of a number of different energies is dispersed at various angles. The X-rays are detected by means of a scintillation or proportional counter rotated through the range of angles at which the X-rays are diffracted.

In recent years, advances in solid-state detector and multichannel analyzer (MCA) or pulse height analyzer (PHA) technology have permitted the development of relatively small and inexpensive energy-dispersive or non-dispersive X-ray fluorescence analyzers. These systems eliminate the high voltage power, water cooling, and heavy radiation shielding required for standard X-ray tubes by substituting a low-intensity radioactive isotope or low-power X-ray tube as the source of exciting radiation. Detection of all X-ray energies is accomplished simultaneously by means of a solid-state detector and a multichannel analyzer. Because all of the fluorescent radiation passes directly into the solid-state detector rather than being dispersed as in a crystal spectrometer, these systems are commonly termed "non-dispersive." Frequently, the term "energy-dispersive" is applied due to the fact that this system, using the multichannel analyzer, directly detects the various X-ray energies rather than the various wavelengths which are directly detected in a crystal spectrometer. Electronic detection has the advantage of eliminating the moving parts and precise mechanical alignment of a crystal spectrometer and makes a more durable and compact system possible.

A schematic diagram of a typical non-dispersive X-ray fluorescence analyzer system is shown in Figure 1. This system utilizes a radioactive isotope as a source of radiation to excite fluorescence in the samples to be analyzed. The choice of isotope depends upon the material to be studied. The range of X-ray energies comprising the characteristic X-ray spectrum of an element can only be produced by excitation with X-rays of greater energy. However, as the excitation energy increases beyond the minimum required to produce the characteristic fluorescence spectrum, the excitation efficiency decreases. Therefore, a radioactive isotope is typically chosen which produces X-rays only a few thousand electron volts above the characteristic spectrum to be studied.

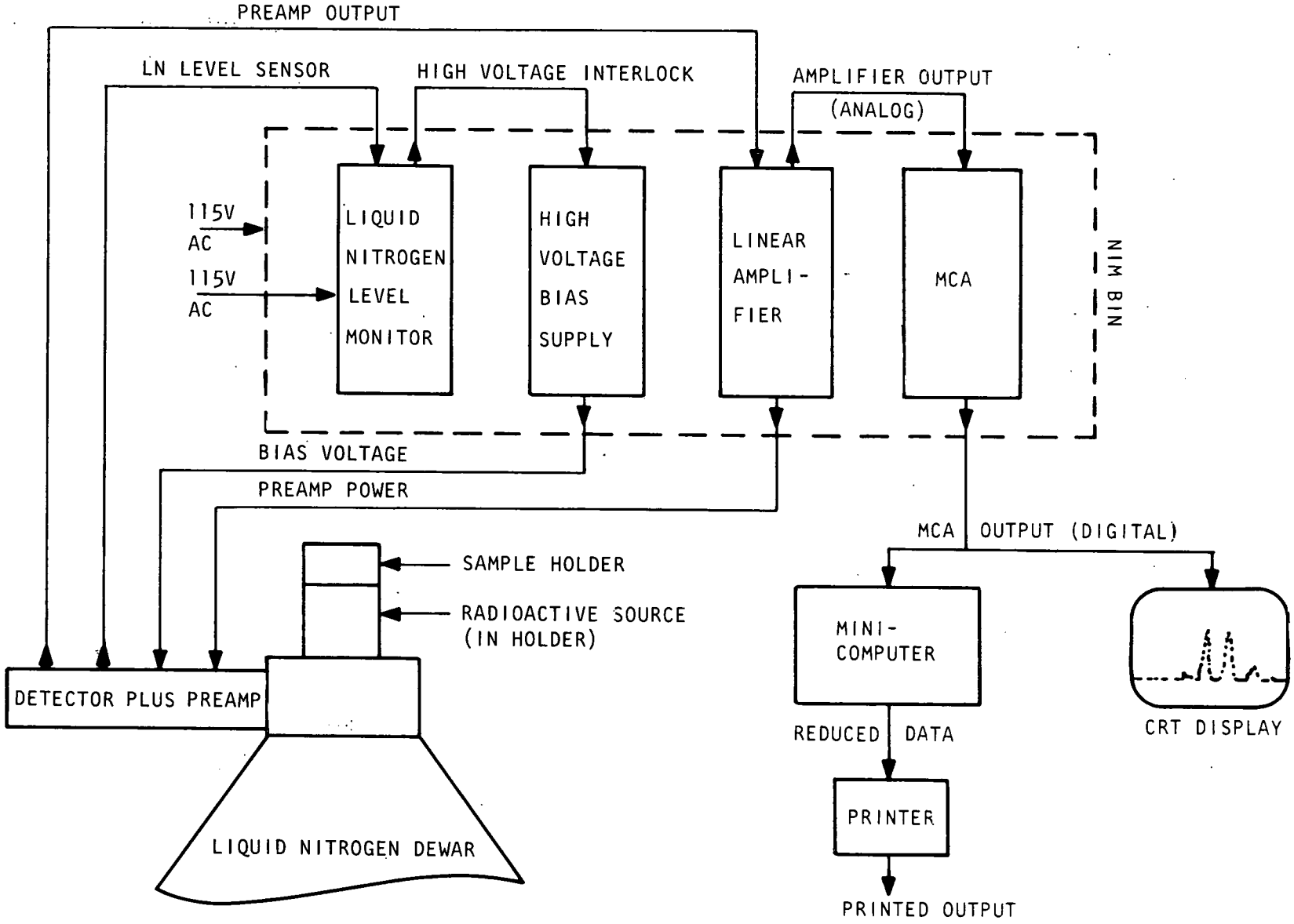

Figure 1. Non-Dispersive X-Ray Fluorescence Analyzer (Schematic)

The detector is a lithium-drifted silicon diode in which the output is amplified by a cryogenic preamplifier utilizing a field effect transistor (FET). X-ray fluorescence photons from a sample pass through the diode detector and produce electron/hole charge carriers (pair production) which are collected by a high bias voltage applied to the diode. The number of charge carriers and, therefore, the magnitude of the resulting voltage pulses, is proportional to the energy of the X-ray photons which produce them. Each pulse is amplified to millivolt levels in the FET preamplifier. Both the silicon diode and the FET are maintained at cryogenic temperatures in a liquid nitrogen dewar. This insures a low level of electronic noise and prevents the physical degradation of the silicon diode that occurs at room temperature. The system may utilize a liquid nitrogen level monitor with an interlock to the high voltage bias supply to prevent operation of the unit in a warm-up condition.

The voltage pulses from the preamp are amplified in a linear amplifier to the level of a few volts and are digitized and counted in the MCA. The MCA distributes the incoming voltage pulses among a number of discrete channels with increasing channel number corresponding to increasing voltage. The pulses are counted as they are accumulated in each channel of the MCA. Since the magnitude of each voltage pulse is a measure of the energy of the X-ray photon that produced it, the contents of a given channel in the MCA represent X-ray fluorescence photons of a given energy. Thus, the total accumulation in all channels of the MCA represents the X-ray spectra from all elements in the sample.

Since all channels of the MCA are counted simultaneously and for the same time, the relative magnitude of the count in each channel represents the relative intensity of the X-ray energies. By suitable calibration and data reduction, the amounts of the elements present in the sample may be determined from this data. Printed output and reduction of the MCA data is provided by a computer or data analyzer through a teletype console or printer. The raw data may be displayed on a cathode ray tube (CRT) display.

The specific system which was purchased and developed for in-process alloy control at Bendix is detailed below.

Radioactive Source:	Cadmium 109, 25 millicurie (925 megadisintegrations/second).
X-Ray Detector:	Ortec, Model 7016-06180, with 6-mm-diameter lithium-drifted silicon diode and 0.025-mm beryllium cryostat window.

Cryogenic Preamplifier:	Ortec, Model 117A.
Amplifier:	Ortec, Model 716A.
High Voltage Bias Supply:	Ortec, Model 459, 3 kV.
Multichannel Analyzer (MCA):	Northern Scientific, Model 633.
Cathode Ray Tube Display:	Northern Scientific, Model 416.
Liquid Nitrogen Level Monitor:	Ortec, Model 717.
Data Reduction and Printout:	Hewlett Packard Minicomputer, Model 2100A, and Scope Data Terminal, Model 200.

The X-ray detector and preamplifier in a 31-liter liquid nitrogen dewar is free-standing, and the Hewlett Packard minicomputer is rack mounted. All other components are contained in a Northern Scientific, Model 106, Nuclear Instrument Module (NIM) Bin. The NIM Bin is rack mounted. Figures 2 and 3 show the system components.

Calibration and Data Reduction

Determination of gold-copper alloy composition from the X-ray data requires two operations: determination of the total counts in each of the characteristic gold and copper peaks chosen for analysis, and comparison of this intensity data to that measured from calibration parts of known composition. The Cu Kα (8.037 keV [1.288 fJ]) and Au Lα (9.711 keV [1.556 fJ]) X-ray energy peaks were chosen for analysis. These are strong peaks which can be accumulated in a reasonable count time and are efficiently excited by the 22.1-keV (3.541 fJ) gamma rays from ^{109}Cd. The peaks are spaced far enough apart to be easily resolvable while readily falling within the range of the MCA. The Cu Kα peak is centered between channels 100 and 101, and the Au Lα is centered on channel 121 with the amplifier gain at 153.2 and proper zero offset adjustment. The high voltage bias on the detector diode is -1500 V. The ^{109}Cd source with 25-millicurie activity was found to excite sufficiently intense fluorescence, even in the relatively small copper peak, to yield statistically meaningful data at 1- to 2-minute count times. Initial attempts using a 2-millicurie (74 megadisintegrations/second) source did not produce usable data even with count times in excess of 8 minutes.

The calibration technique which was developed consists of exposing calibration samples of known alloy composition to the exciting radiation and counting the resulting fluorescent X-rays for a pre-set time of 2 minutes. The 256 channels of MCA data are

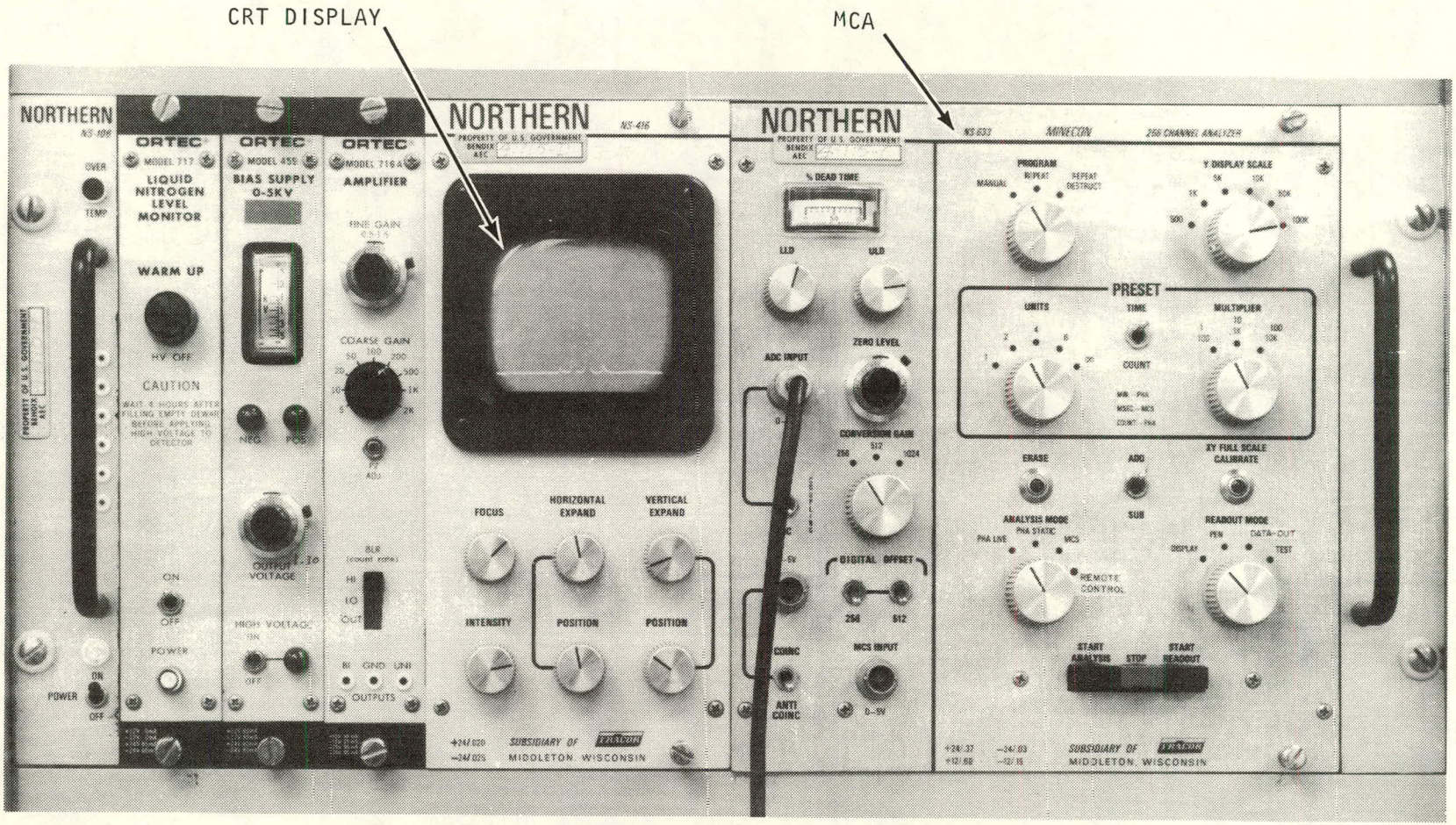

Figure 2. X-Ray Fluorescence System NIM Bin Components

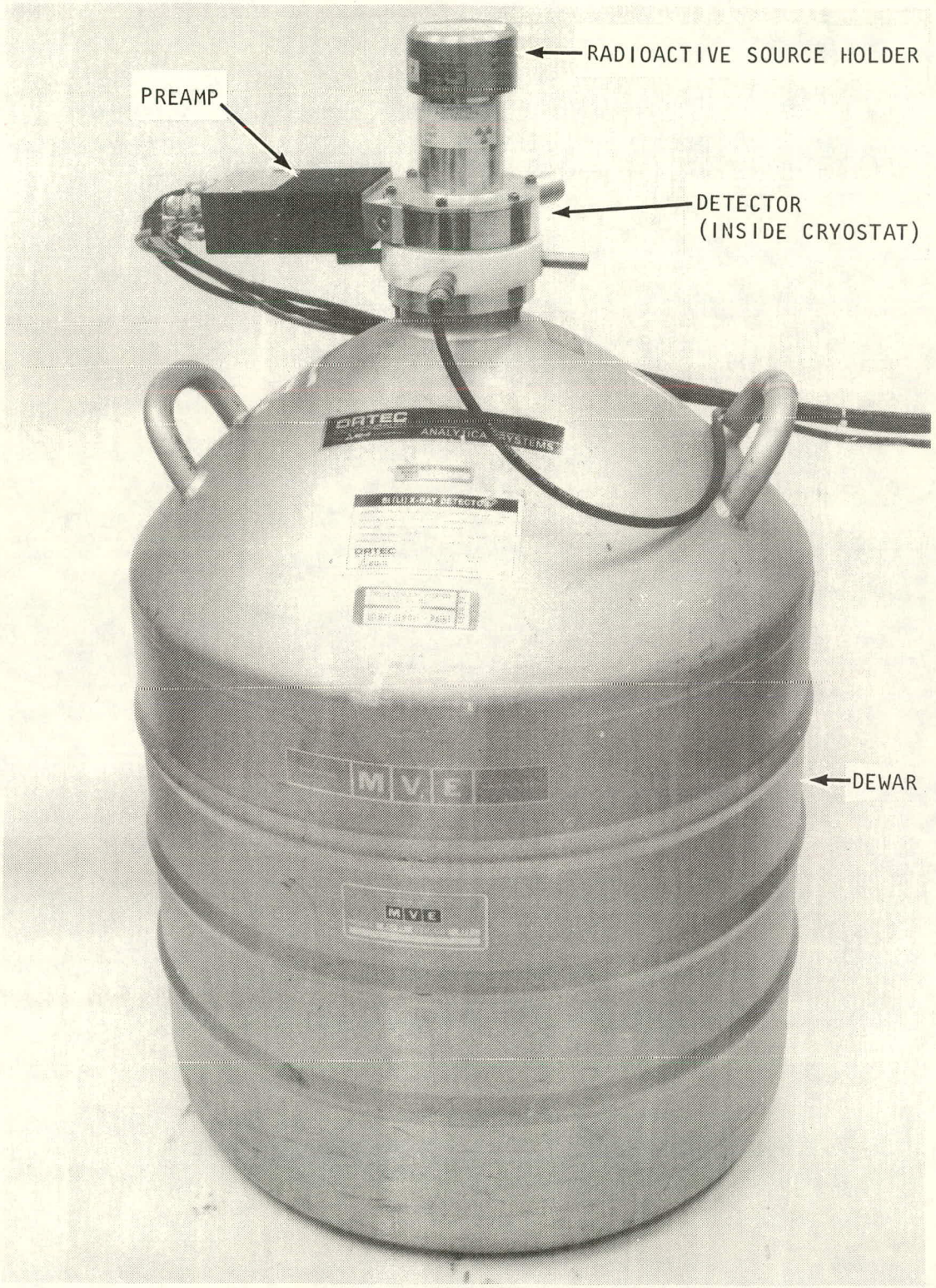

Figure 3. X-Ray Fluorescence System Cryostat Components

read out, and a copper count ratio is defined as the ratio of the count in the Cu Kα peak (background corrected) to the total count in the Cu Kα and Au Lα peaks (background corrected). This is given by

$$R = \frac{C - C_B}{(C - C_B) + (A - A_B)}, \tag{1}$$

where

R = Copper count ratio,

C = Total integrated count in the Cu Kα peak,

C_B = Background over the range of the Cu Kα peak,

A = Total integrated count in the Au Lα peak, and

A_B = Background over the range of the Au Lα peak.

The count ratio is calculated from the MCA data as follows where M is the count for a particular MCA channel and i is the channel number.

$$C = \sum_{i=98}^{103} M_i \quad \text{(summation of channels 98 through 103 of the MCA count data)}, \tag{2}$$

$$C_B = \frac{3}{10}\left(\sum_{i=70}^{79} M_i + \sum_{i=180}^{189} M_i \right), \tag{3}$$

$$A = \sum_{i=117}^{125} M_i, \tag{4}$$

and

$$A_B = \frac{9}{20}\left(\sum_{i=70}^{79} M_i + \sum_{i=180}^{189} M_i \right) . \qquad (5)$$

The limits of summation of both the copper and gold peaks are so chosen that they lie between 1 and 2 times the width of the peak at 1/2 of the maximum value of the peak. The background for a characteristic peak of an element may be defined as the counts which would be accumulated if an identical measurement were made on a sample identical in every way except for the removal of that particular element. This may be approximated in a single measurement by considering the accumulated count in channels which lie on either side of the characteristic peaks of interest and which contain no other characteristic peaks of the elements of the sample. In this case, the background of the copper and gold peaks of interest was approximated by calculating the average count per channel in channels 70 through 79 and 180 through 189 and multiplying this value by the number of channels containing each peak.

The copper count ratio for each calibration sample is calculated and plotted against the known copper content of the sample, and a curve is fitted to the data. The validity of the calibration is a function of the precision of the X-ray measurements on the calibration samples and the accuracy with which the copper content of each calibration sample is known. Since the ratio of copper count to total count is plotted against the weight fraction of copper in the binary alloy, an approximately linear curve is expected, especially in a limited region about the 5 weight percent (w/o) Cu point, with no significant discontinuities or inflections.

Fabrication of calibration samples was first attempted by electroplating thin deposits of gold-copper onto nickel-over-brass substrates using constant reference voltage alloy control. Each potential calibration sample was plated at a different value of reference voltage so that, together, the samples would cover a range from about 2 to 20 w/o copper. Half of each part was subjected to wet chemical analysis while the other half was retained for use as an X-ray standard. Counts were taken on each part, and the copper count ratios were calculated and plotted against the copper contents determined by wet analysis. A second degree polynomial curve was fitted to the data, and the result is shown in Figure 4. Considerable scatter is apparent, with poor approximation to a linear relationship. Since the X-ray count ratios were found to be repeatable, the scatter is attributed to poor alloy composition data. This may be due to non-uniformity in the plated deposits, inaccurate chemical analyses, or both.

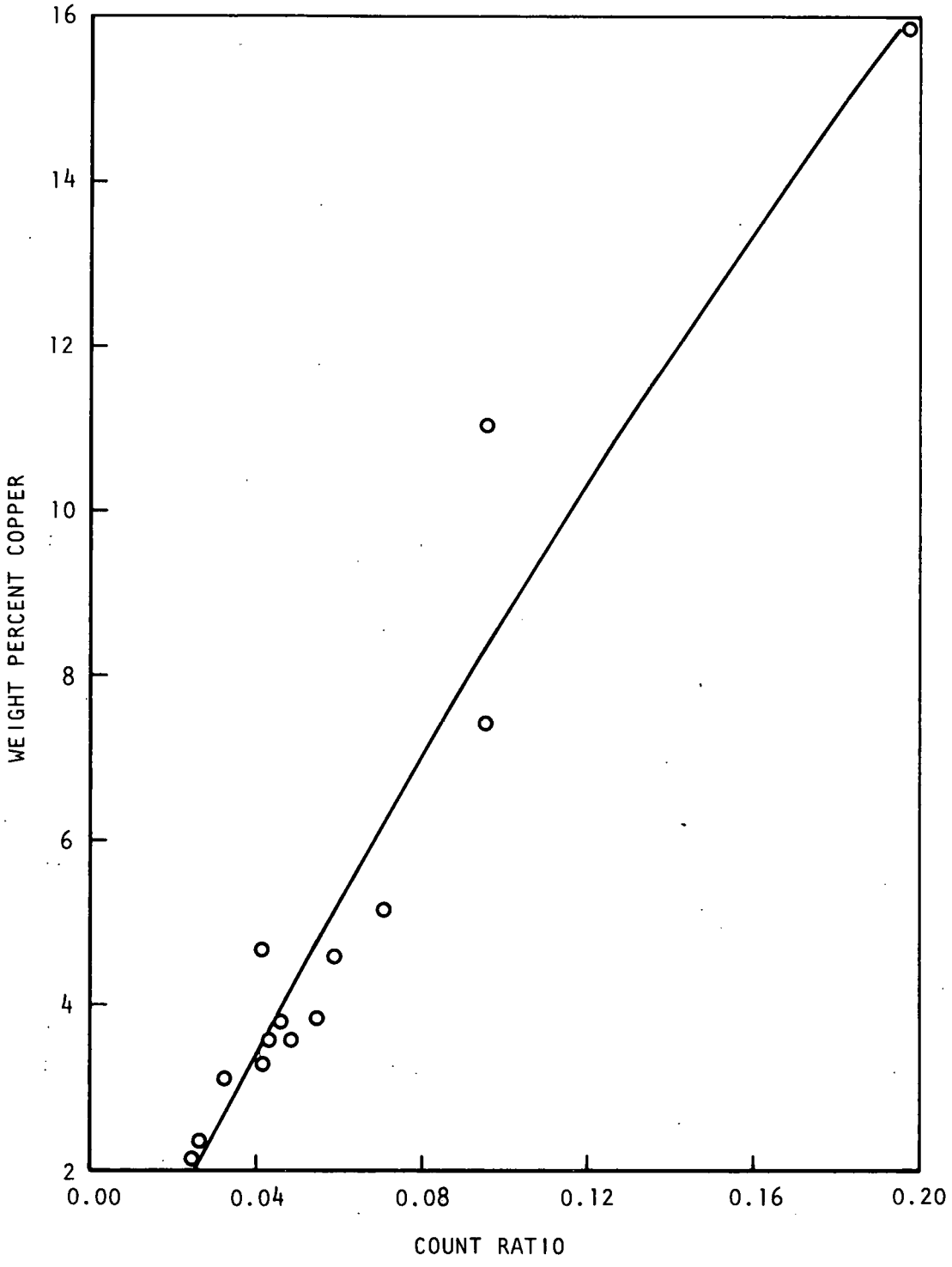

Figure 4. Alloy Versus Count Ratio for Plated Standards

A number of gold-copper calibration standards which had been used for this purpose in similar work at Lawrence Livermore Laboratory were then procured. These samples were circular coupons fabricated by vacuum melting and casting precisely weighed quantities of gold and copper. This technique yielded standards having both precisely known overall alloy composition and excellent compositional uniformity. A plot of copper count ratio versus alloy composition and a second degree polynomial curve fitted to the data from these parts is shown in Figure 5. A very nearly linear fit was achieved, and this curve is presently in use as the calibration curve for gold-copper composition.

Alloy determination of an unknown sample consists of subjecting it to X-ray analysis and calculating the copper count ratio in an identical manner to that for the calibration samples. The alloy composition is then determined by reading the copper content corresponding to this ratio from the calibration curve. In order to facilitate use of the technique, a computer program was developed for the Hewlett Packard Model 2100A minicomputer which prints out the 256 channels of raw data from the MCA, performs data reduction, and determines the weight percent copper from the coefficients of the calibration curve. A representation of a typical printout from the program is shown in Figure 6. The raw data are printed in horizontal lines beginning with MCA channel numbers, which are even multiples of ten. The program will accept up to a third degree polynomial as the calibration curve and the coefficients are designated A_0 through A_3. The weight percent copper is printed along with the maximum and minimum values corresponding to the statistical counting error at the 95 percent confidence level. Also printed is the value of the count ratio and its statistical counting error, the background counts over the range of the gold and copper peaks, the total integrated count in the peaks, and the standard counting error and relative fractional counting error of each of the individual peaks. A discussion of the statistical counting error and its significance is in the Appendix.

In-Process Alloy Control: Precision and Accuracy

The X-ray fluorescence analyzer is now in use as the primary method of in-process alloy control for gold-copper electroplating. Due to compositional variations on a part, the mean of three readings taken at three positions on the part is the value used for process control purposes. The weight density technique continues to be used as a back-up. The overall precision of the X-ray fluorescence technique as determined by the spread in a series of 50 separate and identically performed readings on a sample containing 4.3 w/o copper was found to be ±2.81 percent of the measured value or a spread of ±0.12 w/o copper. The maximum spread calculated from the statistical counting error, representing the theoretical limit of precision, was ±2.56 percent of

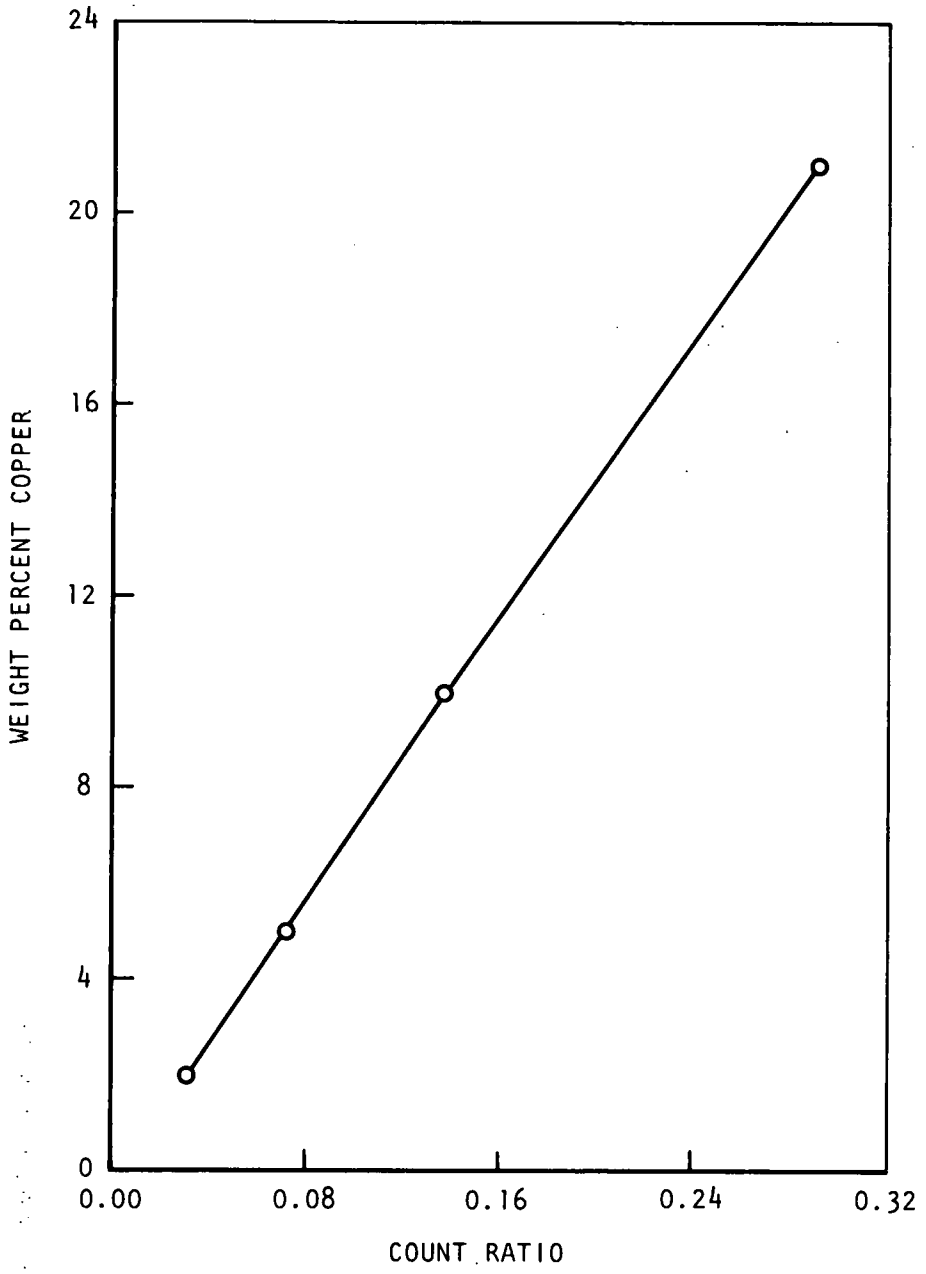

Figure 5. X-Ray Fluorescence Calibration Curve

the measured value. The fact that the measured spread in the readings is only slightly in excess of the statistical counting error suggests a low level of instrumental and operational errors.

A measure of the accuracy of the in-process measurements has been determined by correlation of daily X-ray readings with daily density measurements, and by comparison of X-ray data with electron

Channel Number....	0	1	2	3	4	5	6	7	8	9
0	20000.	2637.	6794.	3863.	1124.	880.	782.	687.	570.	562.
10	513.	474.	395.	424.	407.	425.	409.	385.	369.	411.
20	375.	421.	437.	500.	628.	799.	1097.	1249.	991.	635.
30	418.	357.	314.	305.	279.	271.	293.	279.	280.	265.
40	240.	249.	281.	305.	283.	254.	270.	245.	230.	207.
50	209.	206.	227.	210.	236.	184.	195.	203.	202.	165.
60	192.	187.	189.	184.	216.	223.	181.	204.	193.	204.
70	203.	184.	189.	226.	212.	175.	208.	208.	224.	210.
80	201.	184.	197.	184.	182.	216.	212.	181.	212.	190.
90	197.	229.	251.	269.	303.	349.	571.	1032.	1844.	3199.
100	4454.	4208.	2764.	1776.	1656.	2341.	2839.	2380.	1636.	1030.
110	1008.	1148.	947.	727.	670.	1062.	2639.	6295.	13688.	26618.
120	42989.	54165.	47717.	28071.	11259.	4371.	2617.	2251.	1980.	1710.
130	1294.	875.	635.	578.	619.	966.	1600.	3050.	6158.	11773.
140	20278.	32392.	46492.	55082.	49792.	35454.	20727.	10829.	5762.	3761.
150	2517.	1702.	1071.	737.	602.	481.	437.	458.	440.	523.
160	598.	703.	987.	1458.	2508.	4024.	5928.	7035.	6258.	4314.
170	3271.	3008.	2763.	2102.	1378.	891.	713.	734.	726.	696.
180	545.	494.	423.	408.	387.	380.	388.	434.	469.	448.
190	449.	450.	464.	449.	520.	518.	532.	568.	550.	563.
200	570.	555.	571.	568.	613.	611.	637.	661.	681.	684.
210	716.	754.	750.	732.	708.	747.	785.	712.	776.	823.
220	806.	761.	799.	762.	799.	774.	816.	785.	822.	786.
230	875.	867.	876.	838.	910.	965.	1018.	968.	975.	1081.
240	1128.	1187.	1302.	1181.	1039.	1001.	1075.	1100.	1158.	1241.
250	1475.	1607.	1829.	1991.	2024.	2190.				

AO = -.397735 A1 = 77.513641 A2 = -13.839746 A3 = .000000

WEIGHT PERCENT COPPER = 4.6314 95% CONFIDENCE RANGE = 4.5428 TO 4.7199

CU/CU + AU = .06565 RANGE = .06448 TO .06682
CU BACKGROUND = 1924.50 AU BACKGROUND = 2886.75
CU PEAK = 18245. BACKGROUND ADJUSTED = 16320.50
AU PEAK = 235173. BACKGROUND ADJUSTED = 232286.25
RELATIVE FRACTIONAL COUNTING ERROR (%): CU = 1.74038 AU = .42010 (2 SIGMA)
STANDARD COUNTING ERROR: CU = 284.03876 AU = 975.82739 (2 SIGMA)
XRAY COMPLETE

Figure 6. Representation of Computer Printout of Fluorescence Analysis Data

microprobe analysis data. The comparison of X-ray and density measurements is shown in Table 1, comprising data from plating runs conducted over a 3-month period. The X-ray data correlates well with the daily density values with no consistent bias. All process adjustments were made on the basis of the X-ray values, and all runs met alloy specifications as indicated by post-plate D-test of the process control part by wet chemical and electron microprobe analyses.

It should be noted that the correlation of the daily X-ray and density readings does not give a direct measure of the accuracy of the X-ray method. When properly performed, the density measurement itself is subject to a maximum error of as much as ±0.3 w/o for a 24-hour check. Furthermore, the density reading is the average of an approximately 200-μm-thick (0.008 inch) layer of material, whereas the X-ray fluorescence is generated most strongly within the outer 3 μm (100 μin.) of deposit with no detectable contribution below 15 μm (500 μin.). Therefore, some variation in the readings would be expected due to the fact that different volumes of material are being analyzed even though the measurements are made on the same part at the same time.

A more direct measure of accuracy is the correlation of X-ray data with the post-plate electron microprobe analysis which is considered to be the most accurate technique for determining gold-copper alloy composition presently in use at Bendix. Such a correlation was made and has been previously reported in BDX-613-1593. The data is reproduced here as Figure 7. The continuous trace represents microprobe calibration against alloy standards and is considered more accurate than the MAGIC IV computer analysis indicated by dots. The horizontal dashed lines represent the density measurement and show the thickness of material analyzed by that method. The dip in copper content about one-fourth of the way into the deposit was caused by a malfunctioning temperature controller.

With the exception of the point farthest to the right, the alloy as indicated by X-ray is accurate with respect to the electron microprobe analysis within the previously determined precision of the technique. The discrepancy in the final point is attributable to an edge effect in the microprobe analysis. There is similar agreement with the density measurements except during the period of the controller malfunction. The X-ray readings made just before and just after the malfunction correctly show the 5.6 w/o copper being plated at those times as indicated by microprobe. The copper percentages indicated by density readings made just after the malfunction were significantly lower than those indicated by X-ray, but correctly showed the lower average copper content plated during the period. The apparent discrepancy between the X-ray and density readings is explained by the differing thicknesses of material analyzed by the two techniques.

Table 1. Comparison of In-Process Alloy Measurement Techniques

Run/Bath	Date	[A] Alloy by Density (w/o Cu)	Alloy by X-Ray (w/o Cu) 1	2	3	[B] Average	[B - A] (w/o Cu)
35/49	1/21/76	4.55	4.75	4.78	4.67	4.73	+0.18
	1/22/76	4.80	4.94	4.36	4.72	4.67	-0.13
	1/23/76	5.14	4.70	4.49	4.67	4.62	-0.52
	1/24/76	4.67	4.58	5.03	4.64	4.75	+0.08
	1/25/76	5.36	4.75	4.53	4.72	4.67	-0.69
	1/26/76	4.76	5.21	4.53	4.35	4.70	-0.06
17/52	2/19/76	4.48	4.84	4.55	4.80	4.73	+0.25
	2/20/76	4.96	4.82	4.60	4.70	4.71	-0.25
	2/21/76	4.59	4.21	4.16	4.43	4.27	-0.32
	2/22/76	5.10	4.77	4.69	4.86	4.77	-0.33
	2/23/76	4.93	4.63	4.63	4.73	4.66	-0.27
18/52	2/28/76	5.20	4.91	4.89	4.86	4.89	-0.31
	2/29/76	4.81	4.47	4.59	4.47	4.51	-0.30
	3/1/76	5.07	4.71	4.80	4.64	4.72	-0.35
	3/2/76	4.80	5.05	4.89	5.18	5.04	+0.24
	3/3/76	5.33	4.82	4.98	5.13	4.98	-0.35
22/52	4/23/76	4.96	5.00	4.90	4.97	4.96	0.00
	4/24/76	4.45	4.48	4.45	4.40	4.44	-0.01

ACCOMPLISHMENTS

A source-excited, non-dispersive X-ray fluorescence analyzer was procured and developed for in-process determination of the alloy composition of electroplated gold-copper. This nondestructive technique was shown to be both fast and reliable. An overall precision of ±0.12 w/o in the indicated alloy composition was achieved, and accuracy with respect to electron microprobe analysis data was demonstrated. The technique has been incorporated as the primary method of in-process control of gold-copper plating and replaces a mass density technique which had significant limitations.

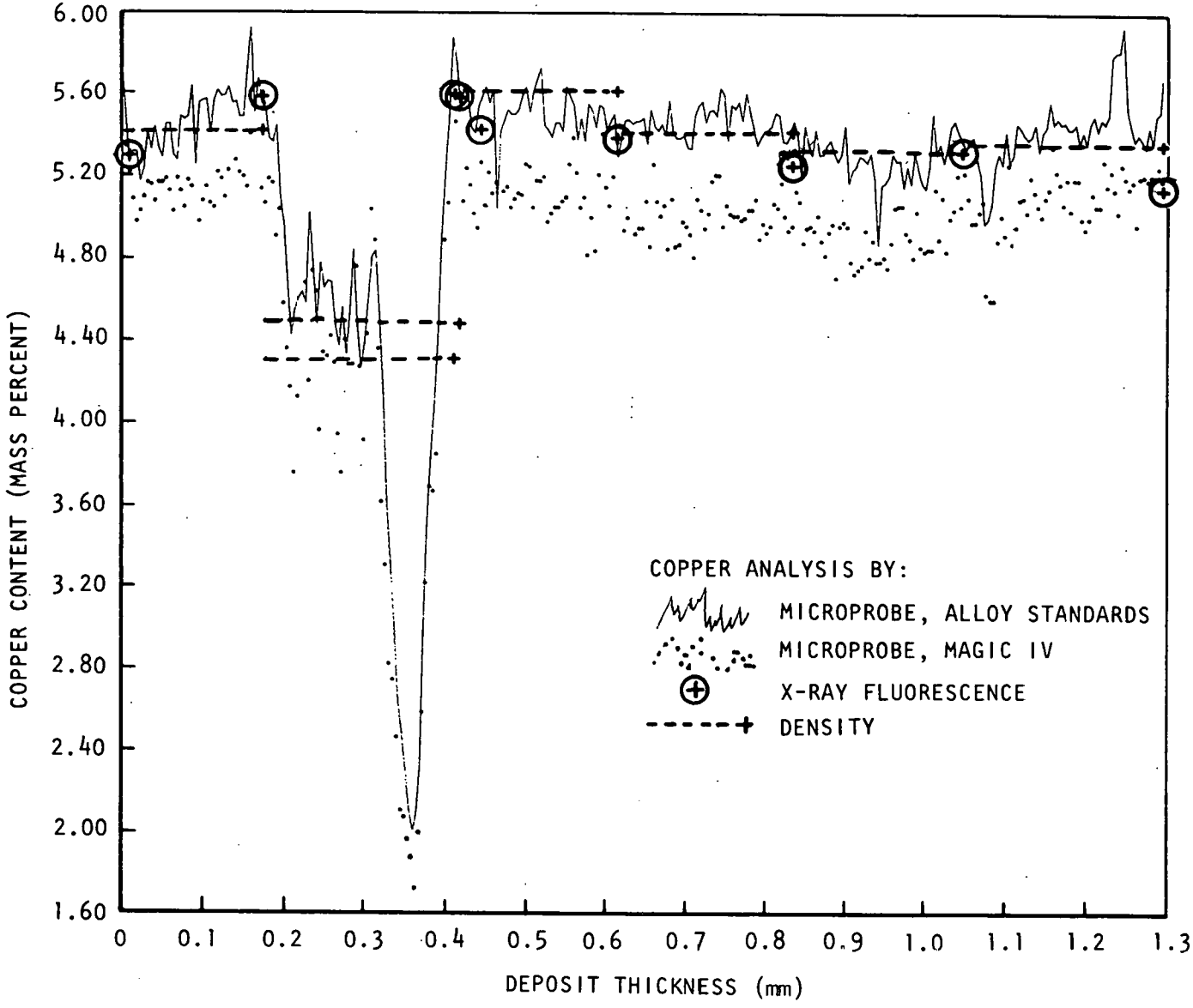

Figure 7. Alloy Composition Versus Increasing Deposit Thickness for Run 31, Bath 49

BIBLIOGRAPHY

Adler, I., *X-Ray Emission Spectrography in Geology.* New York: Elsevier Publishing Company, 1966.

Bertin, E. P., *Principles and Practice of X-Ray Spectrometric Analysis.* New York: Plenum Press, 1970.

Cullity, B. D., *Elements of X-Ray Diffraction.* Reading, Massachusetts: Addison-Wesley Publishing Company, 1956.

Jenkins, R. and Devries, J. L., *Practical X-Ray Spectrometry.* New York: Springer-Verlag, 1967.

Müller, Rudolf O., *Spectrochemical Analysis By X-Ray Fluorescence.* New York: Plenum Press, 1972.

Ortec Operating and Service Manuals, Ortec, Inc., Oak Ridge, Tennessee.

Russ, J. C., *Energy Dispersion X-Ray Analysis: X-Ray and Electron Probe Analysis.* Philadelphia: American Society for Testing and Materials, 1970.

Appendix A

COUNTING STATISTICS

The emission of X-ray fluorescence photons is, like radioactive decay, a random process. That is, the individual photons are emitted by atoms in the sample with a random distribution in time. Consequently, if it were possible to make a series of X-ray counts under identical and theoretically ideal conditions, assuming absolutely no instrumental, operational, or other errors of any kind, the successive accumulated counts would not be the same even though they were made during identical finite counting intervals. This spread in the measured values is called the "counting error" and represents the theoretical limit of precision of a series of measurements. Errors in actual measurements made under real conditions would be expected to be in excess of this theoretical lower limit. The counting error may be precisely calculated and is useful as a standard against which to evaluate the actual precision achieved in a series of measurements.

For n separate X-ray intensity measurements yielding N_1, N_2, N_3,..N_n accumulated counts, the specific values of N can be plotted against the number of times that those values were measured during the n readings. A curve could then be fitted to the points. For large n, this curve would closely approach a Gaussian distribution centered about $\bar{N}$ the mean of the measurements of N. The area under the curve bounded by any two values of N represents the probability that a single measurement of N will fall between those values. For a Gaussian distribution, the area within one standard deviation of the mean ($\pm 1\sigma$) is 68.3 percent of the total area under the curve. The areas bounded by $\pm 2\sigma$, $\pm 3\sigma$, and $\pm 4\sigma$ are 95.4 percent, 99.7 percent, and 99.9 percent respectively. The limits of the value of N between which a given measurement may be expected to fall with a given probability represent the "confidence level" of the measurement. For example, X-ray data may be reported with a $\pm 2\sigma$ tolerance. Since this represents approximately 95 percent of the area under the curve, the data are said to be reported at the 95 percent confidence level. This may be interpreted to mean that there is a 95 percent probability that a single measurement of N will fall within the limits $\bar{N} \pm 2\sigma$. In practice, however, N rather than $\bar{N}$ is known and the data are reported as $N \pm 2\sigma$, the single measured value N with its 2σ tolerance. Since it may generally be assumed that the 2σ associated with the single reading N differs little from the 2σ associated with the mean $\bar{N}$, it is concluded that there is approximately a 95 percent probability that the mean or "true" value $\bar{N}$ falls within $N \pm 2\sigma$.

The ratio of the standard deviation to the measured value is termed the relative standard deviation or coefficient of variation ε and is given by

$$\varepsilon = \frac{\sigma}{N}. \qquad \text{(A-1)}$$

The standard deviation and coefficient of variation of the sum or difference of a series of n measurements are given by

$$\sigma = \sqrt{\sigma_1^2 + \sigma_2^2 + \ldots + \sigma_n^2} \qquad \text{(A-2)}$$

and

$$\varepsilon = \frac{\sqrt{\sigma_1^2 + \sigma_2^2 + \ldots + \sigma_n^2}}{N_1 \pm N_2 \pm \ldots \pm N_n}. \qquad \text{(A-3)}$$

For the product or quotient of a pair of measurements N_1 and N_2

$$\sigma = N_1 N_2^{\pm 1} \sqrt{\left(\frac{\sigma_1}{N_1}\right)^2 + \left(\frac{\sigma_2}{N_2}\right)^2} = N_1 N_2^{\pm 1} \sqrt{\varepsilon_1^2 + \varepsilon_2^2} \qquad \text{(A-4)}$$

and

$$\varepsilon = \sqrt{\varepsilon_1^2 + \varepsilon_2^2}. \qquad \text{(A-5)}$$

The standard deviation specifically associated with the counting error is commonly called the standard counting error. It has been established empirically, and may be shown theoretically, that the numerical value of the standard counting error for a single measurement of N counts is given by

$$\sigma_N = \sqrt{N}. \qquad \text{(A-6)}$$

The relative standard deviation specifically associated with the counting error is commonly called the relative fractional counting error. Its value for a measurement of N counts may be calculated from Equations A-1 and A-6 as follows:

$$\varepsilon_N = \frac{\sigma_N}{N} = \frac{\sqrt{N}}{N} = \frac{1}{\sqrt{N}}. \qquad \text{(A-7)}$$

For the case of N counts corrected for background, from Equation A-2

$$\sigma_N = \sqrt{\sigma_P^2 + \sigma_B^2}, \qquad \text{(A-8)}$$

where

σ_P = Standard counting error of the peak of interest and

σ_B = Standard counting error of the background over the range of the peak of interest.

Thus, substituting,

$$\sigma_N = \sqrt{\left(N_P^{1/2}\right)^2 + \left(N_B^{1/2}\right)^2} = \sqrt{N_P + N_B}, \qquad \text{(A-9)}$$

where

N_P = Number of counts in the peak and

N_B = Number of counts in the background over the range of the peak.

From Equation A-3, the relative fractional counting error for this case is given by

$$\varepsilon_N = \frac{\sqrt{N_P + N_B}}{N_P - N_B}. \qquad \text{(A-10)}$$

In Figure 6, the relative fractional counting error and the standard counting error for the individual gold and copper peaks are calculated from Equations A-9 and A-10, with $2\sigma_N$ and $2\varepsilon_N$ representing the 95 percent confidence level.

An expression for the uncertainty in the count ratio and the corresponding weight percent copper reading due to the counting error may be calculated using Equations A-3 and A-5. The count ratio has previously been defined as

$$R = \frac{C - C_B}{C - C_B + A - A_B}, \qquad \text{(A-11)}$$

where (in terms of the notation used in this appendix)

C and C_B are N_P and N_B for the copper peak and

A and A_B are N_P and N_B for the gold peak.

This may be considered as the quotient of two measurements:

$$R = \frac{N_1}{N_2}, \qquad \text{(A-12)}$$

where

$N_1 = C - C_B$ and

$N_2 = C - C_B + A - A_B$.

From Equation A-3, the relative fractional counting error of N_1 is

$$\varepsilon_1 = \frac{\sqrt{C + C_B}}{C - C_B}, \qquad \text{(A-13)}$$

and the relative fractional counting error of N_2 is

$$\varepsilon_2 = \frac{\sqrt{C + C_B + A + A_B}}{C - C_B + A - A_B}. \qquad \text{(A-14)}$$

Then, from Equation A-5,

$$\varepsilon_R = \sqrt{\varepsilon_1^2 + \varepsilon_2^2} = \sqrt{\left(\frac{C + C_B}{(C - C_B)^2}\right) + \left(\frac{C + C_B + A + A_B}{(C - C_B + A - A_B)^2}\right)} \qquad \text{(A-15)}$$

The range in the count ratio shown in Figure 6 is calculated from this expression with $2\varepsilon_R$ representing the 95 percent confidence level.

Finally, it should be noted that whereas the magnitude of the standard counting error increases with increasing N (increasing count time), the value of the relative fractional counting error decreases. Taking the simple case of the standard counting error of the measurement of a single peak, background corrected,

$$\sigma_N = \sqrt{N_P + N_B} = \sqrt{R_P T + R_B T} = \sqrt{T} \times \sqrt{R_P + R_B}, \qquad \text{(A-16)}$$

where

R_P = Count rate at the peak of interest,

R_B = Count rate of the background, and

T = Count time.

Since R_P and R_B are constant over the count time T, then the magnitude of σ_N increases with increasing T. Considering the relative fractional counting error,

$$\varepsilon_N = \frac{\sqrt{N_P + N_B}}{N_P - N_B} = \frac{\sqrt{R_P T + R_B T}}{R_P T - R_B T} = \frac{\sqrt{R_P + R_B}}{\sqrt{T}(R_P - R_B)}. \qquad \text{(A-17)}$$

Since R_P and R_B are constant, the relative fractional counting error decreases with increasing T. Since ε_N is inversely proportional to the square root of T, it is obvious that the relative counting error may be decreased to whatever level desired by an appropriate increase in count time. Decreasing the error by 1/2, for example, requires a 4X increase in count time.

DISTRIBUTION

	Copy
R. Bulcock, ERDA-KCAO	1
F. B. Baker, LASL	2
T. A. Sandford, LASL	3
D. J. Sandstrom, LASL	4
C. Sanford, LLL	5
E. A. Thompson/P. M. Naillon, LLL	6
H. J. Weisner, LLL	7
J. J. West, LLL	8
J. D. Corey, D/554, BD50	9-10
L. Stratton, D/554, 2C44	11-13
R. P. Frohmberg, D/800, 2A39	14
B. T. Lampe, D/812, 2A27	15
R. A. Hines, D/812, 2A27	16
J. R. Lembke, D/812, 2A27	17
M. L. Smith, D/812, 2A27	18
D. L. Stoltz, D/814, 2C43	19
G. L. MacCurdy, D/816, SC-3	20
W. G. Cooper, D/821, 2A36	21
W. B. Harding, D/821, 2A36	22
D. M. Starks, D/821, 2A36	23
R. E. Kessler, D/865, 2C40	24-25

BDX-613-1716 PDO 6984809

DETERMINATION OF GOLD-COPPER ALLOY COMPOSITION BY X-RAY FLUORESCENCE ANALYSIS, D. M. Starks, D/812, UNCLAS Final, September 1977

The development of a technique for in-process determination of the composition of electroplated gold-copper by X-ray fluorescence analysis is described. The principle of X-ray fluorescence spectroscopy and the operation of a source-excited, non-dispersive X-ray fluorescence analyzer are discussed. A calibration technique which makes use of standards with known alloy composition is

SPECIAL PROJECTS: X-Ray Fluorescence Spectroscopy

DETERMINATION OF GOLD-COPPER ALLOY COMPOSITION BY X-RAY FLUORESCENCE ANALYSIS, D. M. Starks, D/812, UNCLAS Final, PDO 6984809, BDX-613-1716, September 1977

The development of a technique for in-process determination of the composition of electroplated gold-copper by X-ray fluorescence analysis is described. The principle of X-ray fluorescence spectroscopy and the operation of a source-excited, non-dispersive X-ray fluorescence analyzer are discussed. A calibration technique which makes use of standards with known alloy composition is

DETERMINATION OF GOLD-COPPER ALLOY COMPOSITION BY X-RAY FLUORESCENCE ANALYSIS, D. M. Starks, D/812, UNCLAS Final, PDO 6984809, BDX-613-1716, September 1977

The development of a technique for in-process determination of the composition of electroplated gold-copper by X-ray fluorescence analysis is described. The principle of X-ray fluorescence spectroscopy and the operation of a source-excited, non-dispersive X-ray fluorescence analyzer are discussed. A calibration technique which makes use of standards with known alloy composition is

presented, and the use of this technique, along with the precision and accuracy achieved, for in-process analysis is discussed.

presented, and the use of this technique, along with the precision and accuracy achieved, for in-process analysis is discussed.

presented, and the use of this technique, along with the precision and accuracy achieved, for in-process analysis is discussed.